European Journal of Neuroscience, Vol. 14, pp. 1784–1792, 2001

Changes in P2X receptor responses of sensory neurons from $P2X_3$-deficient mice

Yu Zhong,[1] Philip M. Dunn,[1] Michelle Bardini,[1] Anthony P. D. W. Ford,[2] Debra A. Cockayne[2] and Geoffrey Burnstock[1]

[1]Autonomic Neuroscience Institute, Department of Anatomy and Developmental Biology, Royal Free and University College Medical School, Rowland Hill Street, London, NW3 2PF, UK
[2]Roche Bioscience, Palo Alto, CA 94304, USA

Keywords: ATP, DRG, nodose, knock-out

Abstract

Dorsal root ganglion (DRG) neurons respond to ATP with transient, persistent or biphasic inward currents. In contrast, the ATP responses in nodose neurons are persistent. These sustained currents are also heterogeneous, with one component being accounted for by $P2X_{2/3}$ receptors, and the residual response probably mediated by $P2X_2$ receptors, although the direct evidence for this has been lacking. In the present study, we examined the P2X receptors on DRG and nodose neurons from $P2X_3$-deficient ($P2X_3^{-/-}$) mice, using whole cell voltage-clamp recording and immunohistochemistry. We found that all $P2X_3^{-/-}$ DRG neurons lacked rapidly desensitizing response to ATP, and both DRG and nodose neurons from $P2X_3$-null mutant mice no longer responded to α,β-methylene ATP (αβmeATP). In contrast, ATP evoked persistent inward current in 12% of DRG neurons and 84% of nodose neurons from $P2X_3^{-/-}$ mice. This retained persistent response to ATP on nodose neurons had an EC_{50} for ATP of 77 μM, was antagonized by Cibacron blue and pyridoxal-5-phosphate-6-azophenyl-2′,4′-disulphonic acid, potentiated by Zn^{2+} and acidification, but not enhanced by ivermectin or diinosine pentaphosphate. 2′,3′-*O*-Trinitrophenyl-ATP antagonized this response with an IC_{50} of 8 μM. All these properties are consistent with those of recombinant $P2X_2$ homomeric receptors. Furthermore, specific $P2X_2$ receptor immunoreactivity detected in wild-type sensory neurons was unaltered in null mutant mice. Therefore, the αβmeATP-insensitive persistent responses on nodose neurons are likely to be mediated by $P2X_2$ homomers, which contribute to 60% of currents evoked by 100 μM ATP in the wild type.

Introduction

P2X receptors are formed from a family of seven homologous subunits ($P2X_{1–7}$), which can combine to form homomeric and heteromeric receptors (for review see Ralevic & Burnstock, 1998). In the rat, high levels of $P2X_3$ expression are found in a subpopulation of primary afferent neurons, including those of dorsal root ganglia (DRG), trigeminal, and nodose ganglia (Chen *et al*., 1995; Cook *et al*., 1997; Vulchanova *et al*., 1997, 1998; Bradbury *et al*., 1998). Intense $P2X_3$ immunoreactivity is also present in the peripheral and central terminals of these sensory neurons (Cook *et al*., 1997; Vulchanova *et al*., 1997, 1998; Bradbury *et al*., 1998; Llewellyn-Smith & Burnstock, 1998; Novakovic *et al*., 1998; Cockayne *et al*., 2000). This highly selective expression pattern has led to the view that $P2X_3$ subunits may play important roles in sensory transmission (see Burnstock, 2000).

In addition to $P2X_3$, low levels of mRNA transcripts and proteins for $P2X_{1–2}$, $P2X_{4–6}$, have also been detected in sensory neurons of the rat (Collo *et al*., 1996; Xiang *et al*., 1998). The colocalization of some of these subunits suggests that mixed populations of receptors may be present in the same neurons, arising from different combinations of P2X subunits (Lewis *et al*., 1995; Collo *et al*., 1996; Vulchanova *et al*., 1997; Barden & Bennett, 2000). Indeed, the time course of the response to ATP and its analogues in these neurons is quite variable. In trigeminal and DRG neurons, three types of responses have been observed: transient, sustained and biphasic (having both transient and sustained components) (Cook *et al*., 1997; Burgard *et al*., 1999; Grubb & Evans, 1999; Li *et al*., 1999; Ueno *et al*., 1999; Dunn *et al*., 2000). The presence of homomeric $P2X_3$ receptors and heteromeric $P2X_{2/3}$ receptors has been suggested (Burgard *et al*., 1999; Grubb & Evans, 1999), although the additional presence of some $P2X_2$ receptors cannot be excluded. The possibility that some transient responses may be mediated by $P2X_1$ receptors has also been suggested (Petruska *et al*., 2000). In contrast, rat nodose neurons respond to ATP and its analogue α,β-methylene ATP (αβmeATP) with sustained responses. However, in these neurons, biphasic inhibition curves were obtained with 2′,3′-*O*-trinitrophenyl-ATP (TNP-ATP), an antagonist which is selective for $P2X_1$, $P2X_3$ and $P2X_{2/3}$ receptors. This indicates the presence of multiple receptors most probably formed from $P2X_2$ and $P2X_3$ subunits in the forms of $2_n3_{(N-n)}$, where N = the total number of subunits in the receptor (Thomas *et al*., 1998). The lack of subunit selective agonists/antagonists has so far prevented the direct pharmacological characterization of this mixed population of receptors.

Recently, we have generated $P2X_3$-deficient mice (Cockayne *et al*., 2000), to study the roles of P2X receptors containing the $P2X_3$ subunit. Here, we report the changes in the responses of DRG and nodose neurons after disruption of $P2X_3$ receptor expression. We have also characterized, using pharmacological and immunohisto-

Correspondence: Dr Yu Zhong, as above.
E-mail: y.zhong@ucl.ac.uk

Received 20 February 2001, revised 17 September 2001, accepted 16 October 2001

chemical techniques, the P2X receptors retained in nodose neurons of these mutant mice. By removing the major P2X subunits expressed in these neurons, the presence of low levels of other subunits might become more apparent. Preliminary accounts of some of these data have appeared in Abstract form (Zhong *et al*., 2000a).

Methods

Generation of $P2X_3$ knock-out mice

$P2X_3$-deficient mice were generated by deleting 1 kb of the $P2X_3$ gene encompassing exon 1 and the initiating ATG (Cockayne *et al*, 2000). Briefly, the $P2X_3$ gene was cloned from a mouse ES-129/Ola P1 genomic library (Genome Systems, St. Louis, MO, USA). The $P2X_3$ targeting vector included a total of 6.3 kb of genomic sequence, a loxP flanked neomycin resistance gene (Neo), and the HSV-TK gene. Homologous recombination between the targeting vector and the wild-type $P2X_3$ allele results in deletion of a 1.0-kb region of the $P2X_3$ gene, and replacement of this sequence with the loxP flanked Neo gene. A Not 1 linearized targeting vector was electroporated into 129Ola-derived E14-1 embryonic stem cells, and clones were selected in 310 mg/mL active G418 (Gibco BRL, Gaithersburg, MD, USA) and 2 μM gancyclovir (Roche Pharmaceuticals, Nutley, NJ, USA). Southern blot analysis using a 140-bp 5′ flanking region probe identified positive clones with the predicted 3.0 kb and 1.5 kb *Eco*RI fragments diagnostic of the wild-type and mutant $P2X_3$ alleles. Targeted clones were injected into C57BL/6 (Harlan, Indianapolis, IN, USA) blastocysts, and chimeras were established. Germline transmission of the targeted allele was established by mating chimeras to C57BL/6 (Harlan) mice. All mice analyzed in this study have the genetic background 129Ola × C57BL/6 (Harlan), and were derived from either heterozygous F_1 crosses or homozygous F_2 crosses.

Cell culture

Single neurons from nodose ganglia and DRG of adult wild-type and null mutant mice (6–8-month-old) were enzymatically isolated as described previously (Zhong *et al*., 1998). Briefly, mice were killed by inhalation of a rising concentration of CO_2 and death was confirmed by cardiac haemorrhage. The nodose ganglia and DRG were rapidly dissected out, and placed in Leibovitz's L-15 medium (Life Technologies, Paisley, UK). The ganglia were then desheathed, cut and incubated in 4 mL Ca^{2+}/Mg^{2+}-free Hanks' Balanced Salt Solution with 10 mM HEPES buffer (pH 7.0) (HBSS; Life Technologies) containing 1.5 mg/ml collagenase (Class-II, Worthington Biochemical Corporation, Reading, UK) and 6 mg/ml bovine serum albumin (Sigma, Poole, UK) at 37 °C for 40 min. The ganglia were then incubated with 4 mL HBSS containing 1 mg/ml trypsin (Sigma) at 37 °C for 20 min. The solution was replaced with 3 mL growth medium comprising of L-15 medium supplemented with 10% bovine serum, 50 ng/ml nerve growth factor, 0.2% $NaHCO_3$, 5.5 mg/ml glucose, 200 IU/ml penicillin and 200 μg/ml streptomycin. The ganglia were dissociated into single neurons by gentle trituration. The cells were then centrifuged at 160 ***g*** (900 r.p.m.) for 5 min, resuspended in 1 mL growth medium and plated onto 35-mm Petri dishes coated with 10 μg/ml laminin (Sigma). Cells were maintained at 37 °C in a humidified atmosphere containing 5% CO_2, and used after 2–48 h.

Electrophysiology

Whole cell voltage-clamp recording was carried out at room temperature using an Axopatch 200B amplifier (Axon Instruments, Foster City, CA, USA). Membrane potential was held at –60 mV. External solution contained (mM): NaCl 154, KCl 4.7, $MgCl_2$ 1.2, $CaCl_2$ 2.5, HEPES 10, glucose 5.6, the pH was adjusted to 7.4 using NaOH. Recording electrodes (resistance 2–4 MΩ) were filled with internal solution which contained (mM): citric acid 56, $MgCl_2$ 3, CsCl 10, NaCl 10, HEPES 40, EGTA 0.1, tetraethylammonium chloride 10, and the pH adjusted to 7.2 using CsOH (total Cs^+ concentration 170 mM). The composition of this solution was chosen to minimize complications arising from the secondary activation of any potassium or chloride currents. Series resistance compensation of 72–75% was used in all recordings. The threshold for minimum response detectable was set as 20 pA. Data were acquired using pCLAMP software (Axon Instruments). Signals were filtered at 2 kHz (–3 dB frequency, Bessel filter, 80 dB/decade).

For nodose neurons, drugs were applied by gravity flow from independent reservoirs through a 7-barrel manifold comprising fused glass capillaries inserted into a common outlet tube (tip diameter of ~200 μm) which was placed approximately 200 μm from the cell (Dunn *et al*., 1996). One barrel was used to apply drug-free solution to enable rapid termination of drug application. Solution exchange measured by changes in open tip current was complete in 200 ms; however, complete exchange of solution around an intact cell was considerably slower (≤ 1 s). For DRG neurons, drugs were applied through a similar 4-barrel manifold, controlled by computer driven solenoid valves. The exchange of solution around the cell was complete in ≤ 100 ms. The intervals between agonist application were 2 min for nodose, and 3.5 min for DRG neurons, respectively, which were sufficient to achieve reproducible responses.

All data are expressed as the mean ± SEM. Statistical analysis (Student's *t*-test) was performed using Prism v2 (Graphpad, San Diego, CA, USA). Concentration-response data were fitted with the Hill equation: $Y = A/[1 + (K/X)^n]$, where A is the maximum effect, K is the EC_{50}, and n is the Hill coefficient, using Prism v2, Graphpad. The combined data from the given number of cells were fitted, and the results are presented as values ± SE, determined by the fitting routine. Traces were acquired using Fetchex (pCLAMP software) and plotted using Origin (Microcal, Northampton, MA, USA). ATP, αβmeATP and Cibacron blue were obtained from Sigma Chemical Co (Poole, UK). Pyridoxal-5-phosphate-6-azophenyl-2′,4′-disulphonic acid was purchased from Tocris Cookson Ltd (Bristol, UK). 2′,3′-*O*-Trinitrophenyl-ATP was obtained from Molecular Probes (Leiden, Netherlands). Solutions (10 and 100 mM) of ATP and other drugs were prepared using deionized water and stored frozen. All drugs were then diluted in extracellular bathing solution to the final concentration.

Immunohistochemistry

Adult wild-type and null mutant mice were killed as described above and the nodose and DRG were dissected out. These ganglia were rapidly frozen by immersion in isopentane at –70 °C for 2 min. The sections were cut to 10 μm thickness using a cryostat, thaw-mounted on gelatine-coated slides and air-dried at room temperature.

Polyclonal antisera for $P2X_{1-7}$ receptors were generated and characterized as previously described (Xiang *et al*., 1998; Oglesby *et al*., 1999). Antibodies against rat $P2X_{1-6}$ receptors were applied to the tissue and visualized using the avidin-biotin (ABC) technique (Llewellyn-Smith *et al*., 1993; Zhong *et al*., 1998). Briefly, the sections were fixed in 4% formaldehyde (in 0.1 M phosphate buffer) containing 0.03% picric acid (pH 7.4) for 10 min. Endogenous peroxidase was blocked with 50% methanol containing 0.4% hydrogen peroxide (H_2O_2) for 10 min. Non-specific binding was blocked by a 20-min incubation with 10% normal horse serum (NHS) (Life Technologies) in phosphate-buffered saline (PBS) containing 0.05% merthiolate (Sigma). The sections were incubated with the primary antibodies

diluted to 2.5 μg/ml (determined as optimal by previous titrations) with 10% NHS in PBS containing 0.05% Merthiolate overnight. Subsequently the sections were incubated with biotinylated donkey antirabbit IgG (Jackson Immunoresearch, PA. USA) diluted 1 : 500 in 1% NHS in PBS containing 0.05% Merthiolate for 1 h, followed by the incubation with ExtrAvidin-horseradish peroxidase (Sigma) diluted 1 : 1500 in PBS containing 0.05% Merthiolate for 1 h. All incubations were held at room temperature and separated by 3 × 5-min washes in PBS. Finally, freshly prepared colour reaction mixture containing 0.5% 3,3′-diaminobenzidine, 0.1 M sodium phosphate, 0.004% NH_4Cl, 0.2% glucose, 0.04% nickel ammonium sulphate and 0.1% glucose oxidase were applied to the sections for 5 min. The sections were then washed, dehydrated, cleared in xylene and mounted using Eukitt (BDH, Poole, UK).

Results

Immunohistochemistry

Antibodies raised against the C-terminus of rat $P2X_{1–6}$ subunits were used on mouse DRG and nodose ganglia. Strong $P2X_3$ immunoreactivity was observed in many small diameter neurons in DRG and nodose ganglia of wild-type mice (Fig. 1A and E). Less intense staining was present in medium diameter neurons, while most large cells showed little $P2X_3$ immunoreactivity. In sensory ganglia from $P2X_3$ knockout mice, specific $P2X_3$-immunostaining was totally absent (Fig. 1B and F). Specific membrane-bound $P2X_2$ immunoreactivity was present in many DRG and nodose neurons from the wild-type mice (Fig. 1C and G) and appeared to be qualitatively unchanged in the null mutant (Fig. 1D and H). In addition, $P2X_5$ and $P2X_6$ immunoreactivity was present in similarly low levels in DRG and nodose ganglia from wild-type and mutant mice (data not shown), while immunoreactivity for $P2X_1$, $P2X_4$ or $P2X_7$ was not detected in mouse sensory ganglia (data not shown).

Electrophysiology

DRG neurons

In wild-type mice, 10 μM ATP evoked a rapidly desensitizing inward current in 42% (26/61) of neurons, with the average amplitude being 0.41 ± 0.09 nA (Fig. 2A). In 21% (13/61) of neurons, ATP evoked a sustained current of 0.51 ± 0.19 nA (Fig. 2B). A further 5% (3/61) of neurons gave biphasic responses with both transient and sustained components. Comparable transient, sustained or biphasic responses were evoked in these neurons by 30 μM αβmeATP. All $P2X_3^{+/+}$ neurons tested (40/40) responded to 100 μM γ-aminobutyric acid (GABA); while 31% (9/29) responded to 5 μM capsaicin. There did not appear to be any correlation between sensitivity to capsaicin and ATP**.**

In the $P2X_3$-deficient mice, application of either ATP (10–300 μM) or αβmeATP (30–100 μM) failed to produce a rapidly desensitizing inward current in DRG neurons (49 cells tested) (Fig. 2C). Sustained responses to ATP were observed in 12% (6/49) of neurons, while no slowly desensitizing response was evoked by 30 μM αβmeATP (Fig. 2D). As in wild-type neurons, all cells tested (41/41) responded to 100 μM GABA, and 23% (6/26) responded to 5 μM capsaicin**.**

Nodose neurons

Whole cell responses. In wild-type mice, of the 46 nodose neurons tested with both ATP and αβmeATP (10–100 μM), 96% (44/46) responded to ATP, and 43/46 of the cells also responded to αβmeATP. Amongst the cells that responded to both agonists, 39 neurons gave a persistent response, one cell gave a transient response, and three cells gave biphasic responses with both transient and sustained components (Fig. 3A and B). The amplitude of the persistent response to 100 μM ATP was 5.2 ± 0.5 nA (mean ± SEM, $n = 25$), which was significantly greater than the response to 100 μM αβmeATP (3.1 ± 0.4 nA, $n = 18$, $P < 0.05$).

In null mutant mice, none of the nodose neurons tested ($n = 12$) responded to 100 μM αβmeATP, yet they all gave a persistent response to 30 μM ATP (Fig. 3C). The proportion of neurons responding to ATP (43/51, 84%) was not significantly different ($P > 0.1$) from that of the wild type. However, the mean amplitude of the persistent response to 100 μM ATP (3.2 ± 0.6 nA, $n = 26$) was significantly ($P < 0.05$) smaller than that observed for $P2X_3^{+/+}$ neurons (5.2 ± 0.5 nA).

These results indicate that mixed populations of P2X receptors are present on wild-type mouse nodose neurons. Consequently, in $P2X_3^{+/+}$ nodose neurons, αβmeATP evoked a significantly lower maximum response than that of ATP, and the disruption of the $P2X_3$ gene only reduced the amplitude of the ATP response by 40%. This suggests that a significant proportion of the ATP current in wild-type nodose neurons is mediated through an αβmeATP-insensitive receptor. Hence, we sought to examine the pharmacological properties of this αβmeATP-insensitive receptor present in $P2X_3^{-/-}$ nodose neurons.

Concentration-response curves for agonists. Rapid application of ATP, but not αβmeATP, evoked persistent responses in $P2X_3^{-/-}$ nodose neurons. Fitting the Hill equation to the concentration–response relationship for ATP yielded an EC_{50} of 77 μM (log EC_{50} = –4.11 ± 0.04, $n = 5$) and a Hill coefficient of 2.1 (Fig. 4).

In wild-type mice, the concentration–response curve for αβmeATP on nodose neurons had an EC_{50} of 35 μM ($\log EC_{50}$ = –4.45 ± 0.07, $n = 5$), and a Hill coefficient of 1.5 (Fig. 4). As ATP activated at least two populations of P2X receptors on $P2X_3^{+/+}$ nodose neurons, we attempted to fit its concentration–response curve with the two-component Hill equation, assuming equal proportions of both components. Using the EC_{50} value for one component of 77 μM (as previously determined from the $P2X_3^{-/-}$ neurons), this gave an EC_{50} for the second component of 12 μM ($n = 5$).

Effect of antagonists. Cibacron blue is a potent antagonist of neuronal $P2X_2$ receptors (Zhong *et al*., 1998). In $P2X_3^{-/-}$ nodose neurons, the response to ATP (30 μM) was inhibited by Cibacron blue (10 μM) to 11 ± 1% of the control ($n = 5$), after a 2-min preincubation. The response recovered to 107 ± 10% of the control ($n = 4$) 2 min after washing out the antagonist (Fig. 5A and B).

Pyridoxal-5-phosphate-6-azophenyl-2′,4′-disulphonic acid (PPADS) produced a time- and concentration-dependent antagonism of the response to ATP at neuronal $P2X_2$ receptors (Zhong *et al*., 1998). In $P2X_3^{-/-}$ nodose neurons, following a 4-min preincubation with 1 μM of PPADS, the response to ATP was reduced by approximately 40%. In the presence of 10 μM PPADS, the response to ATP was almost completely abolished (Fig. 5C). There was little recovery 4 min after washing to remove PPADS ($n = 4$)**.**

The P2X antagonist 2′,3′-O-trinitrophenyl-ATP (TNP-ATP) displays 1000 fold higher potency on recombinant $P2X_1$, $P2X_3$ and $P2X_{2/3}$ receptors over $P2X_2$ receptors (Virginio *et al*., 1998; Dunn *et al*., 2000). On $P2X_3^{+/+}$ nodose neurons, TNP-ATP inhibited the response to αβmeATP (30 μM) with an IC_{50} of 11 ± 2 nM ($n = 4$, Fig. 6). In contrast, the response evoked by ATP (30 μM) from $P2X_3^{-/-}$ nodose neurons was approximately 1000 times less sensitive to TNP-ATP (IC_{50} = 7.9 ± 0.8 μM, $n = 4$). We then tested the sensitivity of the ATP response in wild-type neurons to 1 μM TNP-

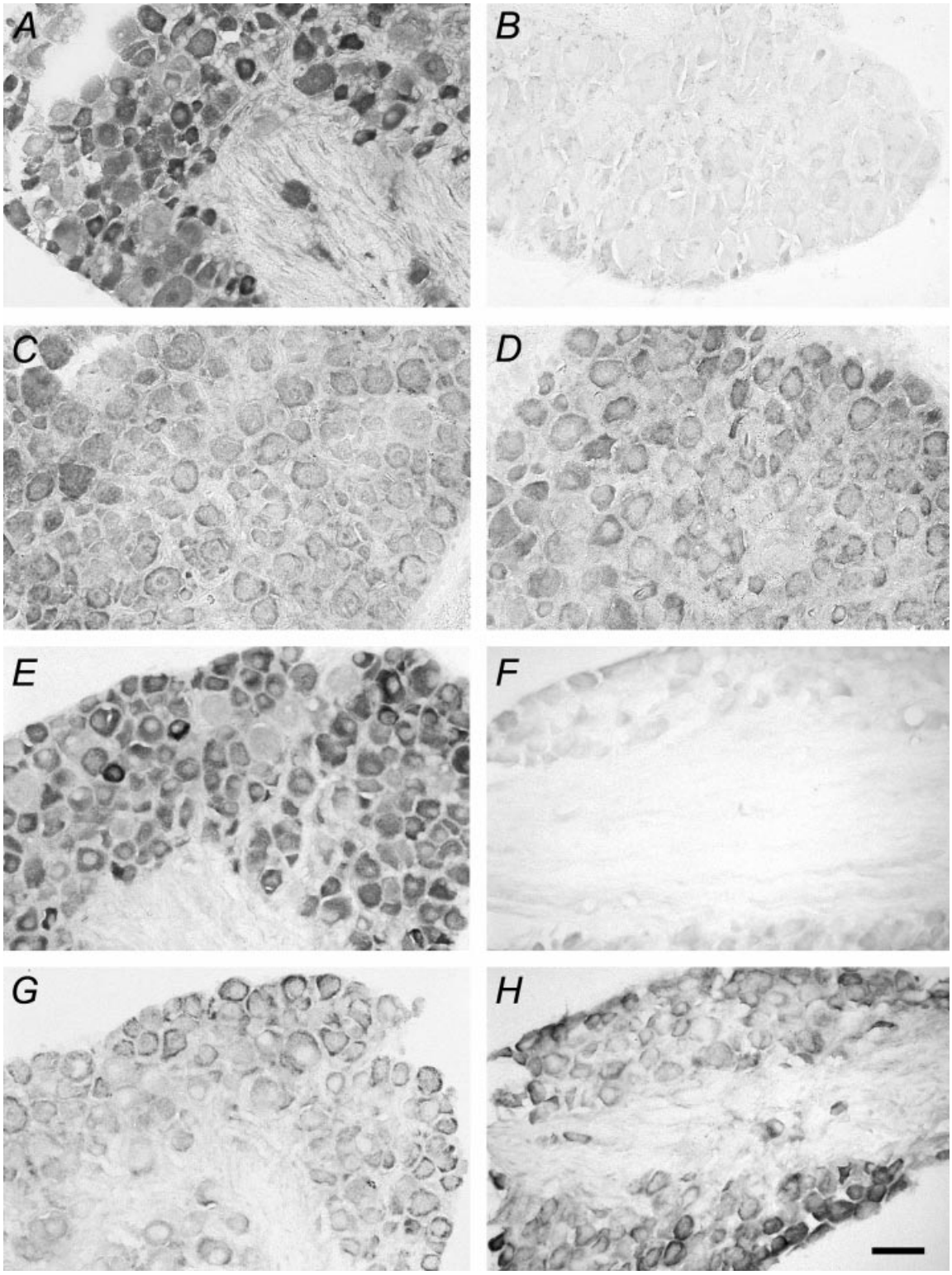

FIG. 1. $P2X_2$ and $P2X_3$ immunoreactivity in mouse sensory ganglia. Dorsal root (A–D) and nodose ganglia (E–H) sections from wild-type (A, C, E and G) and $P2X_3$-null mutant (B, D, F and H) mice were examined using antibodies raised against peptide sequences of the C-termini of rat $P2X_2$ or $P2X_3$ subunits. Specific $P2X_3$ immunoreactivity was observed in sensory ganglion neurons of wild-type mice, with many small diameter neurons showing intense labelling (A and E). This $P2X_3$ immunoreactivity was absent in $P2X_3$-deficient mice (B and F). By contrast, the specific $P2X_2$ immunoreactivity seen in many wild-type DRG and nodose ganglia (C and G) remained unchanged in $P2X_3^{-/-}$ mice (D and H). Scale bar, 50 μm.

ATP (a concentration which abolished the response to αβmeATP in $P2X_3^{+/+}$ neurons, but had no effect on the ATP response in $P2X_3^{-/-}$ neurons). In agreement with the findings of Thomas *et al*. (1998) studying rat nodose neurons, this concentration of TNP-ATP produced some antagonism, but the extent of the inhibition varied considerably from cell to cell (between 25 and 75%, $n = 4$).

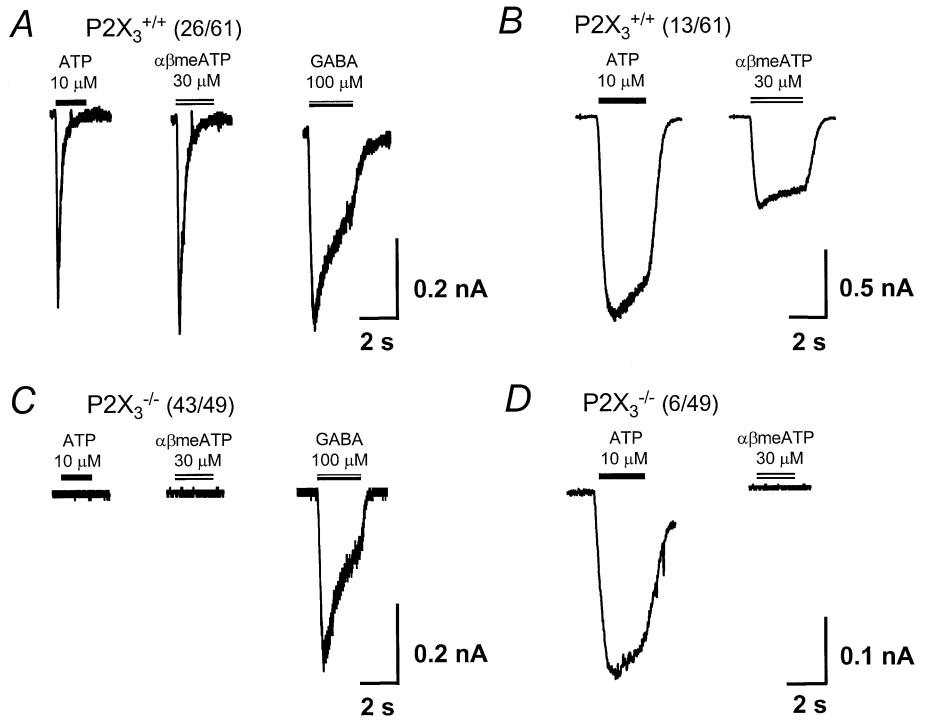

FIG. 2. Responses to αβmeATP, ATP and GABA in dorsal root ganglion neurons from wild-type and $P2X_3$-null mutant mice. (A) Representative traces of the rapidly desensitizing inward current to ATP (10 μM) and αβmeATP (30 μM) recorded in 43% of $P2X_3^{+/+}$ DRG neurons. All wild-type DRG neurons tested responded to GABA (100 μM). (B) 22% of $P2X_3^{+/+}$ DRG neurons showed a slowly desensitizing response to ATP (10 μM) and αβmeATP (30 μM). (C) The majority (88%) of $P2X_3^{-/-}$ DRG neurons gave no response to ATP or αβmeATP (at concentrations up to 300 μM). However, all cells tested responded to GABA (100 μM). (D) 12% of $P2X_3^{-/-}$ DRG neurons responded to ATP (10 μM) with slowly desensitizing responses, but no current was evoked by αβmeATP (30 μM). Cells were voltage clamped at –60 mV. Traces shown in each panel are from a single neuron of the appropriate type. Numbers in brackets indicate the fraction of cells giving the type of response illustrated. The horizontal bars above the traces indicate the duration of agonist application.

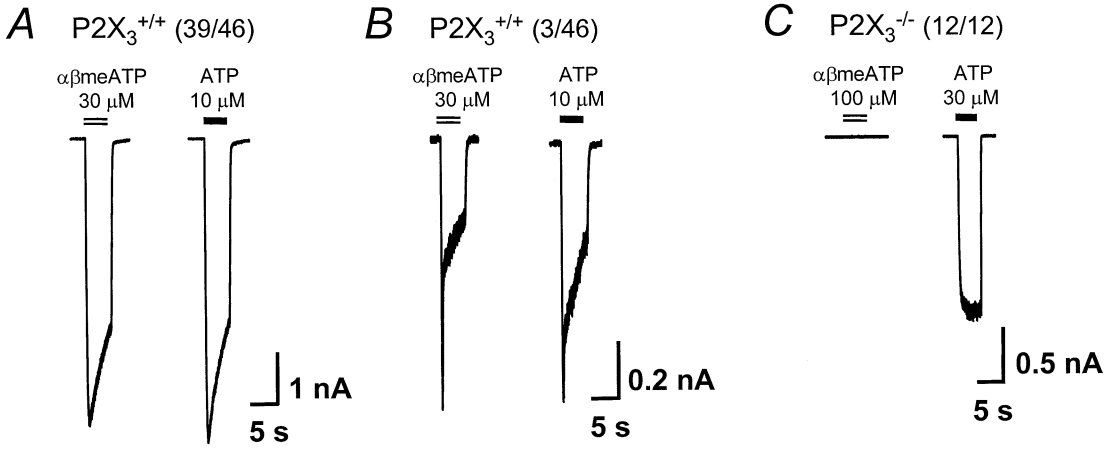

FIG. 3. Responses to αβmeATP and ATP in nodose neurons of wild-type and $P2X_3$-null mutant mice. (A) Representative traces of persistent responses to ATP (10 μM) and αβmeATP (30 μM) recorded in 85% of $P2X_3^{+/+}$ nodose neurons. (B) In 7% of $P2X_3^{+/+}$ nodose neurons, biphasic responses to ATP and αβmeATP were encountered. (C) In this series of experiments, none of the 12 $P2X_3^{-/-}$ nodose neurons tested responded to αβmeATP (100 μM), but they all gave a persistent response to ATP. Cells were voltage clamped at –60 mV. Traces shown in each panel are from a single neuron of the appropriate type. Numbers in brackets indicate the fraction of cells giving the type of response illustrated. The horizontal bars above the traces indicate the duration of agonist application.

Effect of allosteric modulators. Zn^{2+} and H^+ have potent modulatory effects on some P2X receptors (for review see North & Surprenant, 2000). On $P2X_3^{-/-}$ nodose neurons, coapplication of Zn^{2+} (10 μM) enhanced the response to ATP (30 μM) to 224 ± 15% of the control ($n = 5$), and its effect was completely reversible. Lowering the extracellular pH from 7.4 to 6.8 potentiated the response to 30 μM ATP to 229 ± 15% of the control ($n = 5$), and shifted the concentration–response curve for ATP to the left by approximately 0.26 log unit. This was similar to the shift produced by 10 μM Zn^{2+} (data not shown).

The action of ATP at receptors containing the $P2X_4$ subunit can be selectively potentiated by ivermectin (Khakh *et al.*, 1999) and diinosine pentaphosphate (Ip_5I) (King *et al.*, 1999). After a 2-min preincubation with 1 μM ivermectin, the currents evoked by ATP (100 μM) on $P2X_3^{-/-}$ nodose neurons were 99 ± 1% of the control ($n = 5$). Similarly, after a 2-min preincubation with 1 μM Ip_5I, the response to 100 μM ATP was reduced to 92 ± 2% of the control ($n = 6$, $P < 0.01$).

Discussion

Evidence from molecular biology and immunohistochemistry indicate that most P2X subunits are present in sensory neurons (see Dunn *et al.*, 2001 for review). However, functional experiments suggest only a few of these subunits are important. Thus in DRG neurons, the

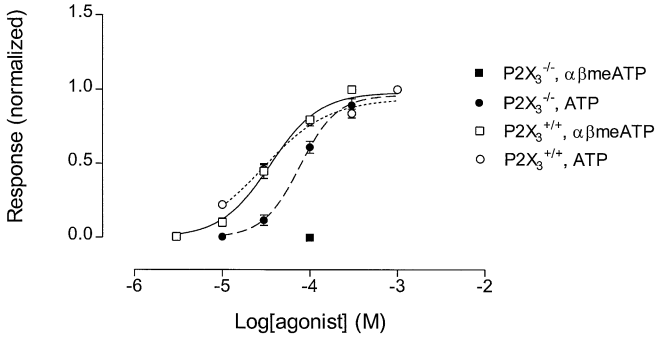

FIG. 4. Concentration-response curves for αβmeATP and ATP on nodose neurons from wild-type and $P2X_3$-null mutant mice. Fitting the Hill equation to the ATP response on $P2X_3^{-/-}$ nodose neurons gave an EC_{50} value of 77 μM and a Hill coefficient of 2.1. In $P2X_3^{+/+}$ nodose neurons, the concentration–response curve for αβmeATP had an EC_{50} of 35 μM, and a Hill coefficient of 1.5, while that for ATP was fitted with the two-component Hill equation, having EC_{50} values of 12 μM and 77 μM (see text for details). Responses to αβmeATP and ATP were normalized to that of 300 μM αβmeATP and 1 mM ATP, respectively. Each data point represents the mean ± SE of 4 or 5 cells.

homomeric $P2X_3$ receptor appears to predominate. In nodose ganglion neurons at least two distinct receptors are present, one activated by αβmeATP, and hence thought to be the heteromeric $P2X_{2/3}$ receptor, the other is insensitive to this agonist and may be the $P2X_2$ homomer. However, the lack of a selective agonist for this receptor has prevented its direct characterization when it coexists with the $P2X_{2/3}$ receptor. In the present study, using $P2X_3$-null mutant mice, we have been able to examine the pharmacological properties of the αβmeATP-insensitive component directly. In addition, we speculated that by deleting one of the major P2X subunits, functional evidence for the presence of other subunits might become more apparent.

Confirmation of the absence of the $P2X_3$ subunit in null mutant mice

In $P2X_3$-null mutant mice, $P2X_3$ immunoreactivity is undetectable in DRG, nodose ganglia, spinal cord and the peripheral terminals of sensory neurons (Fig. 1; also see Cockayne *et al*., 2000). However, neurons that normally express $P2X_3$ are still present with qualitatively similar distribution and patterns of innervation, both peripherally and centrally (Cockayne *et al*., 2000). The absence of $P2X_3$ expression is further confirmed by our functional experiments. No DRG neurons from $P2X_3^{-/-}$ mice responded to ATP with rapidly desensitizing currents, and neither nodose nor DRG neurons from $P2X_3^{-/-}$ mice showed any responsiveness to αβmeATP.

$P2X_3^{-/-}$ nodose neurons retain a $P2X_2$ -like receptor

The mouse P2X subtypes cloned to date, $P2X_3$, $P2X_4$ and $P2X_5$, show >94% identity with rat orthologues at the protein level (Souslova *et al*., 1997; Townsend-Nicholson *et al*., 1999; Cox *et al*., 2001) and appear to exhibit almost identical pharmacological properties. We have previously shown that autonomic ganglion neurons from both rat and mouse possess P2X receptors that exhibit identical pharmacological properties, which are consistent with those of the rat $P2X_2$ homomeric receptor (Zhong *et al*., 2000b). Although some caution is advisable in making direct comparison between the native receptors in the mouse and recombinant rat P2X (rP2X) receptors, the great similarity observed between mouse and rat P2X orthologues permits us to use currently available pharmacological tools (best characterized on rP2X receptors) to study the endogenous P2X receptors in the mouse.

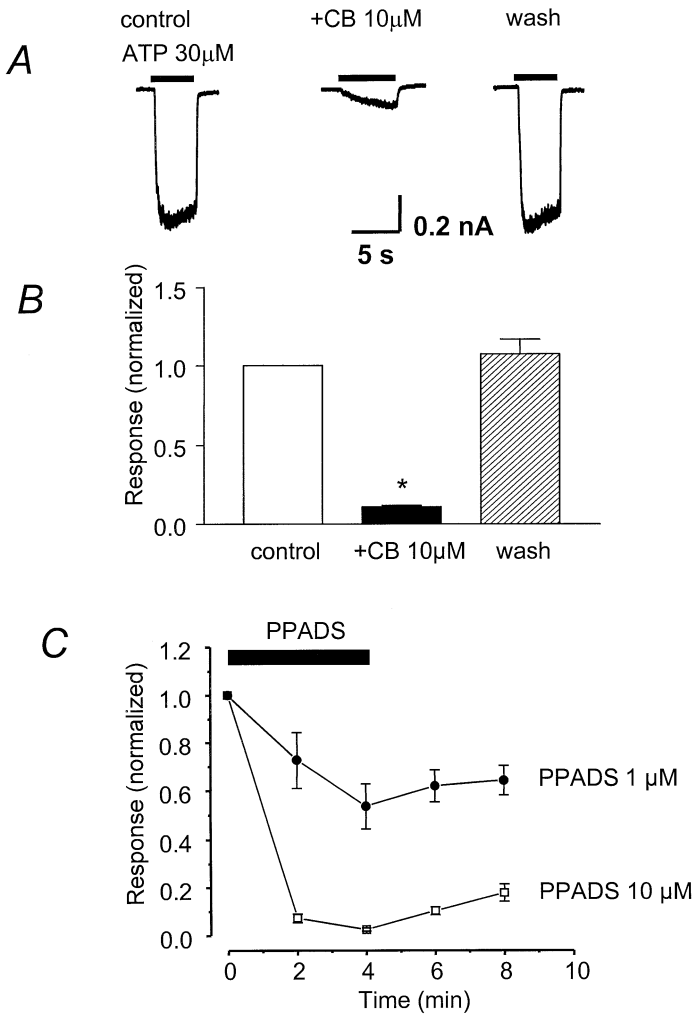

FIG. 5. Antagonism of the ATP response in nodose neurons from $P2X_3$-null mutant mice by Cibacron blue and PPADS. (A) Representative traces showing three consecutive responses from a $P2X_3^{-/-}$ nodose neuron to 30 μM ATP alone, in the presence of 10 μM Cibacron blue (CB, 10 μM), and 2 min after washing out the antagonist. The horizontal bars above the traces indicate the duration of agonist application. (B) Averaged data from 5 neurons. The response to 30 μM ATP was reduced to 11 ± 1% of control ($n = 5$) by Cibacron blue after a 2-min preincubation ($^*P < 0.01$). The response recovered to 107 ± 10% of control ($n = 4$) 2 min after washing out the antagonist. (C) Time and concentration dependent inhibition by PPADS. Responses to 30 μM ATP were recorded at 2 min intervals before, during and following washout of PPADS. Points represent the mean from 4 neurons. Only one concentration of PPADS was tested on each cell. All cells were voltage clamped at –60 mV.

In $P2X_3^{-/-}$ mice, many nodose neurons show specific $P2X_2$ receptor immunoreactivity (Fig. 1), with no detectable levels of $P2X_{1,3,4,7}$ and only low levels of $P2X_5$ and $P2X_6$. In functional experiments, ATP activates a slowly desensitizing inward current with an EC_{50} of 77 μM, while αβmeATP is inactive. These properties are generally in keeping with those of the $rP2X_2$ homomeric receptor (Brake *et al*., 1994). Although the EC_{50} value we obtained for ATP is slightly higher than that of 43 μM obtained for SCG neurons by Khakh *et al*. (1995), there is a wide range of values reported for recombinant $P2X_2$ receptors, ranging from 4 μM (Liu *et al*., 2001) to 60 μM (Brake *et al*., 1994).

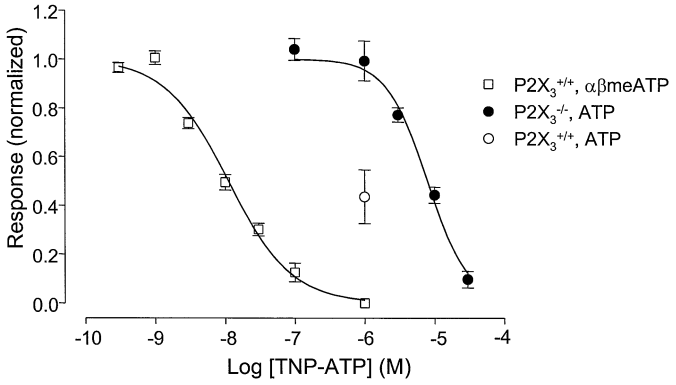

FIG. 6. Concentration inhibition curves by TNP-ATP of agonist responses on nodose neurons of wild-type and $P2X_3$-null mutant mice, using αβmeATP (30 μM) or ATP (30 μM) as the agonist, respectively. TNP-ATP displayed IC_{50} values of 11 nM and 7.9 μM on these two populations of P2X receptors, respectively. In nodose neurons from wild-type mice, the response to ATP (30 μM) was partially inhibited but not abolished by TNP-ATP (1 μM), following a 2-min preincubation. Each data point represents the mean ± SE from 4 or 5 cells.

The ATP response on $P2X_3^{-/-}$ nodose neurons was strongly inhibited by both Cibacron blue and PPADS (10 μM), which are potent antagonists of rat neuronal $P2X_2$ receptors (Zhong *et al*., 1998, 2000b). In addition, the response was potentiated by Zn^{2+} in a similar way to that observed on recombinant $rP2X_2$ receptors (Wildman *et al*., 1998). TNP-ATP inhibited the ATP response in $P2X_3^{-/-}$ nodose neurons with an IC_{50} of 8 μM, which is similar to the value reported for $rP2X_2$ (Virginio *et al*., 1998). Extracellular pH is another tool for discriminating between recombinant P2X receptors, with $P2X_2$ and to a lesser extent $P2X_{2/3}$ and $P2X_{2/6}$ receptors being selectively potentiated by acidification (King *et al*., 1997; Stoop *et al*., 1997; Wildman *et al*., 1999; King *et al*., 2000). The response to ATP on $P2X_3^{-/-}$ nodose neurons was significantly potentiated by the reduction of pH from 7.4 to 6.8. Thus, the sensitivity to pH is again consistent with these currents being accounted for by $P2X_2$ homomers. To further rule out the involvement of $P2X_4$ subunit, we tested the effect of ivermectin and Ip_5I. Ivermectin is a selective potentiator of $P2X_4$ and $P2X_{4/6}$ receptors (with an EC_{50} close to 1 μM), while it is inactive on $P2X_2$ receptors at concentrations up to 10 μM (Khakh *et al*., 1999). Ip_5I, a potent antagonist on $P2X_1$ and $P2X_3$ receptors, potentiates $P2X_4$ receptors with an EC_{50} around 3 nM, yet is inactive on $P2X_2$ at concentrations up to 30 μM (King *et al*., 1999). On $P2X_3^{-/-}$ nodose neurons, neither ivermectin nor Ip_5I (1 μM) produced any enhancement of the ATP response. Thus the ATP response on $P2X_3^{-/-}$ nodose neurons is unlikely to be mediated by $P2X_4$ or $P2X_{4/6}$ receptors. This is consistent with the absence of $P2X_4$ immunoreactivity on mouse sensory ganglia. The detection of low levels of $P2X_5$ and $P2X_6$ immunoreactivity raises the possibility that they may also be involved. However, receptors formed from $P2X_6$ subunits are unlikely because they are resistant to PPADS (Collo *et al*., 1996), yet the ATP response of $P2X_3^{-/-}$ nodose neurons was blockable by PPADS. The properties of $P2X_5$ receptors are similar to that of $P2X_2$ receptors, making it much harder to exclude. Furthermore, the involvement of these subunits in some heteromeric receptors cannot be ruled out. Nevertheless, the simplest explanation which our data would support, is that the response present in $P2X_3^{-/-}$ neurons is mediated by homomeric $P2X_2$ receptors.

Identity of P2X receptors in wild-type mouse nodose and DRG neurons

In $P2X_3^{+/+}$ nodose neurons, the slowly desensitizing current evoked by αβmeATP is consistent with it being conducted by $P2X_{2/3}$ heteromeric receptors. This is further supported by the $P2X_2$- and $P2X_3$-immunoreactivity observed in these ganglia, and is similar to the situation in rat nodose neurons (Lewis *et al*., 1995). In addition, the sensitivity of the αβmeATP response to TNP-ATP is similar to that of recombinant $P2X_{2/3}$ receptors. In wild-type nodose ganglion neurons, ATP activated an additional population of αβmeATP-insensitive receptors, which was much less sensitive to the antagonist TNP-ATP. We speculate that this is the same receptor that is retained in the $P2X_3^{-/-}$ ganglia and which clearly has the phenotype of the $P2X_2$ homomer. This suggests that mouse nodose neurons contain significant proportions of both homomeric $P2X_2$ and heteromeric $P2X_{2/3}$ receptors. Occasionally, we also observed biphasic or transient responses to ATP in approximately 10% of $P2X_3^{+/+}$ nodose neurons. Although both $P2X_1$ and $P2X_3$ homomers may contribute to this transient response, the lack of any detectable $P2X_1$ immunoreactivity and the absence of transient response in $P2X_3^{-/-}$ nodose neurons strongly suggests that $P2X_1$ is not involved in the mouse nodose ganglion.

The three types of currents evoked by ATP in wild-type mouse DRG neurons are very similar to those observed in rat DRG neurons (Burgard *et al*., 1999; Grubb & Evans, 1999). Whereas the presence of $P2X_3$ homomers and $P2X_{2/3}$ heteromers has been suggested in the rat, it is not clear whether $P2X_2$ homomers are also present. In $P2X_3^{-/-}$ DRG neurons, while the rapidly desensitizing response and the sensitivity to αβmeATP are no longer present, approximately 10% cells still responded to ATP with a slowly desensitizing profile. Due to the scarcity of cells showing this type of response, we have not characterized it pharmacologically. However, the available functional and immunohistochemical evidence is consistent with it being the homomeric $P2X_2$ receptor. Thus, in wild-type mouse DRG, in addition to $P2X_3$ homomers and $P2X_{2/3}$ heteromers, $P2X_2$ homomers may also be present at a low level in a small percentage of neurons.

It has been suggested that $P2X_1$ receptors may be responsible for a component of the transient ATP response in some DRG neurons (Petruska *et al*., 2000). Although we cannot rule out the possibility of interspecies differences, or age-dependent changes in receptor expression, the absence of any transient responses in $P2X_3^{-/-}$ mice would argue strongly against this.

Are there compensatory changes?

It is possible that some compensatory changes may occur after the disruption of $P2X_3$ gene expression. We found that responses to GABA and capsaicin appeared to be qualitatively unchanged in $P2X_3$-null mutants, and $P2X_2$ immunoreactivity appeared unaltered in $P2X_3^{-/-}$ neurons. The amplitude of the response to 100 μM ATP in $P2X_3^{-/-}$ nodose neurons (3.2 nA), was smaller than that in the wild-type neurons, consistent with a loss of $P2X_{2/3}$ heteromeric receptors. However, the response was slightly greater than that mediated by the αβmeATP-insensitive receptors in wild-type cells (determined from the difference between the response to ATP and αβmeATP to be 2.1 nA), suggesting that there might be a slight increase in the number of homomeric $P2X_2$ receptors present. Nevertheless, this did not reach statistical significance. Thus there do not appear to be any significant compensatory changes resulting from the null mutation of the $P2X_3$ gene, at least in 6–8-month-old mice.

Implications of findings from $P2X_3$-null mutant mice

Extracellular ATP has been implicated in numerous sensory processes (Burnstock, 2000). Studies on $P2X_3$-deficient mice have pointed out important physiological roles of $P2X_3$-containing receptors in afferent pathways controlling urinary bladder volume reflexes, temperature sensing, and inflammatory pain states (Cockayne *et al*., 2000; Souslova *et al*., 2000). As a significant number of $P2X_2$ and $P2X_{2/3}$ receptors are also present in some sensory neurons including those of the nodose ganglia, it will be important to establish the roles of these other P2X receptors.

Acknowledgements

The authors are grateful to Mr E.W. Moules and Mr T. Robson for excellent technical support, to Mr R. Jordan and Dr C. Orphanides for editorial assistance with the manuscript and to Mr J. Gualix for preparation of Ip_5I. YZ and PMD were supported by Roche Bioscience (Palo Alto, CA, USA).

Abbreviations

ATP, adenosine 5′-triphosphate; DRG, dorsal root ganglion; GABA, γ-aminobutyric acid; HBSS, Ca^{2+}/Mg^{2+}-free Hanks' Balanced Salt Solution with 10 mM HEPES buffer; Ip_5I, diinosine pentaphosphate; αβmeATP, α,β-methylene ATP; mRNA, messenger ribose nucleic acid; NHS, normal horse serum; PBS, phosphate buffered saline; PPADS, pyridoxal-5-phosphate-6-azophenyl-2′,4′-disulphonic acid; TNP-ATP, 2′,3′-O-trinitrophenyl-ATP.

References

Barden, J.A. & Bennett, M.R. (2000) Distribution of P2X purinoceptor clusters on individual rat dorsal root ganglion cells. *Neurosci. Lett.*, **287**, 183–186.

Bradbury, E.J., Burnstock, G. & McMahon, S.B. (1998) The expression of $P2X_3$ purinoceptors in sensory neurons: effects of axotomy and glial-derived neurotrophic factor. *Mol. Cell. Neurosci.*, **12**, 256–268.

Brake, A.J., Wagenbach, M.J. & Julius, D. (1994) New structural motif for ligand-gated ion channels defined by an ionotropic ATP receptor. *Nature*, **371**, 519–523.

Burgard, E.C., Niforatos, W., van Biesen, T., Lynch, K.J., Touma, E., Metzger, R.E., Kowaluk, E.A. & Jarvis, M.F. (1999) P2X receptor-mediated ionic currents in dorsal root ganglion neurons. *J. Neurophysiol.*, **82**, 1590–1598.

Burnstock, G. (2000) P2X receptors in sensory neurones. *Br. J. Anaesth.*, **84**, 476–488.

Chen, C.C., Akopian, A.N., Sivilotti, L., Colquhoun, D., Burnstock, G. & Wood, J.N. (1995) A P2X purinoceptor expressed by a subset of sensory neurons. *Nature*, **377**, 428–431.

Cockayne, D.A., Hamilton, S.G., Zhu, Q.-M., Dunn, P.M., Zhong, Y., Novakovic, S., Malmberg, A.B., Cain, G., Berson, A., Kassotakis, L., Hedley, L., Lachnit, W.G., Burnstock, G., McMahon, S.B. & Ford, A.P.D.W. (2000) Urinary bladder hyporeflexia and reduced pain-related behaviour in $P2X_3$-deficient mice. *Nature*, **407**, 1011–1015.

Collo, G., North, R.A., Kawashima, E., Merlo-Pich, E., Neidhart, S., Surprenant, A. & Buell, G. (1996) Cloning of $P2X_5$ and $P2X_6$ receptors and the distribution and properties of an extended family of ATP-gated ion channels. *J. Neurosci.*, **16**, 2495–2507.

Cook, S.P., Vulchanova, L., Hargreaves, K.M., Elde, R. & McCleskey, E.W. (1997) Distinct ATP receptors on pain-sensing and stretch-sensing neurons. *Nature*, **387**, 505–508.

Cox, J.A., Barmina, O. & Voigt, M.M. (2001) Gene structure, chromosomal localization, cDNA cloning and expression of the mouse ATP-gated ionotropic receptor P2X5 subunit. *Gene*, **270**, 145–152.

Dunn, P.M., Benton, D.C., Campos, R.J., Ganellin, C.R. & Jenkinson, D.H. (1996) Discrimination between subtypes of apamin-sensitive Ca^{2+}-activated K^+ channels by gallamine and a novel bis-quaternary quinolinium cyclophane, UCL 1530. *Br. J. Pharmacol.*, **117**, 35–42.

Dunn, P.M., Liu, M., Zhong, Y., King, B.F. & Burnstock, G. (2000) Diinosine pentaphosphate: an antagonist which discriminates between recombinant $P2X_3$ and $P2X_{2/3}$ receptors and between two P2X receptors in rat sensory neurones. *Br. J. Pharmacol.*, **130**, 1378–1384.

Dunn, P.M., Zhong, Y. & Burnstock, G. (2001) P2X receptors in peripheral neurones. *Prog. Neurobiol.*, **65**, 107–134.

Grubb, B.D. & Evans, R.J. (1999) Characterization of cultured dorsal root ganglion neuron P2X receptors. *Eur. J. Neurosci.*, **11**, 149–154.

Khakh, B.S., Humphrey, P.P.A. & Surprenant, A. (1995) Electrophysiological properties of $P2_X$-purinoceptors in rat superior cervical, nodose and guinea-pig coeliac neurones. *J. Physiol. (Lond)*, **484**, 385–395.

Khakh, B.S., Proctor, W.R., Dunwiddie, T.V., Labarca, C. & Lester, H.A. (1999) Allosteric control of gating and kinetics at $P2X_4$ receptor channels. *J. Neurosci.*, **19**, 7289–7299.

King, B.F., Liu, M., Pintor, J., Gualix, J., Miras-Portugal, M.T. & Burnstock, G. (1999) Diinosine pentaphosphate (IP_5I) is a potent antagonist at recombinant rat $P2X_1$ receptors. *Br. J. Pharmacol.*, **128**, 981–988.

King, B.F., Townsend-Nicholson, A., Wildman, S.S., Thomas, T., Spyer, K.M. & Burnstock, G. (2000) Coexpression of rat $P2X_2$ and $P2X_6$ subunits in *Xenopus* oocytes. *J. Neurosci.*, **20**, 4871–4877.

King, B.F., Wildman, S.S., Ziganshina, L.E., Pintor, J. & Burnstock, G. (1997) Effects of extracellular pH on agonism and antagonism at a recombinant $P2X_2$ receptor. *Br. J. Pharmacol.*, **121**, 1445–1453.

Lewis, C., Neidhart, S., Holy, C., North, R.A., Buell, G. & Surprenant, A. (1995) Coexpression of $P2X_2$ and $P2X_3$ receptor subunits can account for ATP-gated currents in sensory neurons. *Nature*, **377**, 432–435.

Li, C., Peoples, R.W., Lanthorn, T.H., Li, Z.W. & Weight, F.F. (1999) Distinct ATP-activated currents in different types of neurons dissociated from rat dorsal root ganglion. *Neurosci. Lett.*, **263**, 57–60.

Liu, M., King, B.F., Dunn, P.M., Rong, W., Townsend-Nicholson, A. & Burnstock, G. (2001) Coexpression of P2X(3) and P2X(2) receptor subunits in varying amounts generates heterogeneous populations of P2X receptors that evoke a spectrum of agonist responses comparable to that seen in sensory neurons. *J. Pharmacol. Exp. Ther.*, **296**, 1043–1050.

Llewellyn-Smith, I.J. & Burnstock, G. (1998) Ultrastructural localization of $P2X_3$ receptors in rat sensory neurons. *Neuroreport*, **9**, 2245–2250.

Llewellyn-Smith, I.J., Pilowsky, P. & Minson, J.B. (1993) The tungstate-stabilized tetramethylbenzidine reaction for light and electron microscopic immunocytochemistry and for revealing biocytin-filled neurons. *J. Neurosci. Meth.*, **46**, 27–40.

North, R.A. & Surprenant, A. (2000) Pharmacology of cloned P2X receptors. *Annu. Rev. Pharmacol. Toxicol.*, **40**, 563–580.

Novakovic, S.D., Tzoumaka, E., McGivern, J.G., Haraguchi, M., Sangameswaran, L., Gogas, K.R., Eglen, R.M. & Hunter, J.C. (1998) Distribution of the tetrodotoxin-resistant sodium channel PN3 in rat sensory neurons in normal and neuropathic conditions. *J. Neurosci.*, **18**, 2174–2187.

Oglesby, I.B., Lachnit, W.G., Burnstock, G. & Ford, A.P.D.W. (1999) Subunit specificity of polyclonal antisera to the carboxy terminal regions of P2X receptors, $P2X_1$ through $P2X_7$. *Drug Dev. Res.*, **47**, 189–195.

Petruska, J.C., Mena, N., Nakatsuka, T., Cooper, B.Y., Johnson, R.D. & Gu, J.G. (2000) P2X1 receptor subunit immunoreactivity and ATP-evoked fast currents in adult rat dorsal root ganglion neurons. *Neuroreport*, **11**, 3589–3592.

Ralevic, V. & Burnstock, G. (1998) Receptors for purines and pyrimidines. *Pharmacol. Rev.*, **50**, 413–492.

Souslova, V., Cesare, P., Ding, Y., Akopian, A.N., Stanfa, L., Suzuki, R., Carpenter, K., Dickenson, A., Boyce, S., Hill, R., Nebenius-Oosthuizen, D., Smith, A.J.H., Kidd, E. & Wood, J.N. (2000) Warm-coding deficits and aberrant inflammatory pain in mice lacking $P2X_3$ receptors. *Nature*, **407**, 1015–1017.

Souslova, V., Ravenall, S., Fox, M., Wells, D., Wood, J.N. & Akopian, A.N. (1997) Structure and chromosomal mapping of the mouse $P2X_3$ gene. *Gene*, **195**, 101–111.

Stoop, R., Surprenant, A. & North, R.A. (1997) Different sensitivities to pH of ATP-induced currents at four cloned P2X receptors. *J. Neurophysiol.*, **78**, 1837–1840.

Thomas, S., Virginio, C., North, R.A. & Surprenant, A. (1998) The antagonist trinitrophenyl-ATP reveals co-existence of distinct P2X receptor channels in rat nodose neurones. *J. Physiol. (Lond.)*, **509**, 411–417.

Townsend-Nicholson, A., King, B.F., Wildman, S.S. & Burnstock, G. (1999) Molecular cloning, functional characterization and possible cooperativity between the murine $P2X_4$ and $P2X_{4a}$ receptors. *Brain Res. Mol. Brain Res.*, **64**, 246–254.

Ueno, S., Tsuda, M., Iwanaga, T. & Inoue, K. (1999) Cell type-specific ATP-activated responses in rat dorsal root ganglion neurons. *Br. J. Pharmacol.*, **126**, 429–436.

Virginio, C., Robertson, G., Surprenant, A. & North, R.A. (1998) Trinitrophenyl-substituted nucleotides are potent antagonists selective for $P2X_1$, $P2X_3$, and heteromeric $P2X_{2/3}$ receptors. *Mol. Pharmacol.*, **53**, 969–973.

Vulchanova, L., Arvidsson, U., Riedl, M., Wang, J., Buell, G., Surprenant, A., North, R.A. & Elde, R. (1997) Immunocytochemical study of the $P2X_2$ and $P2X_3$ receptor subunits in rat and monkey sensory neurons and their central terminals. *Neuropharmacology*, **36**, 1229–1242.

Vulchanova, L., Riedl, M.S., Shuster, S.J., Stone, L.S., Hargreaves, K.M., Buell, G., Surprenant, A., North, R.A. & Elde, R. (1998) $P2X_3$ is expressed by DRG neurons that terminate in inner lamina II. *Eur. J. Neurosci.*, **10**, 3470–3478.

Wildman, S.S., King, B.F. & Burnstock, G. (1998) Zn^{2+} modulation of ATP-responses at recombinant $P2X_2$ receptors and its dependence on extracellular pH. *Br. J. Pharmacol.*, **123**, 1214–1220.

Wildman, S.S., King, B.F. & Burnstock, G. (1999) Modulatory activity of extracellular H^+ and Zn^{2+} on ATP-responses at $rP2X_1$ and $rP2X_3$ receptors. *Br. J. Pharmacol.*, **128**, 486–492.

Xiang, Z., Bo, X. & Burnstock, G. (1998) Localization of ATP-gated P2X receptor immunoreactivity in rat sensory and sympathetic ganglia. *Neurosci. Lett.*, **256**, 105–108.

Zhong, Y., Dunn, P.M. & Burnstock, G. (2000b) Pharmacological comparison of P2X receptors on rat coeliac, mouse coeliac and mouse pelvic ganglion neurons. *Neuropharmacology*, **39**, 172–180.

Zhong, Y., Dunn, P.M., McMahon, S.B., Burnstock, G., Ford, A.P.D. & Cockayne, D.A. (2000a) Changes in purinoceptor responses in sensory neurones from $P2X_3$ knockout mice. *Soc. Neurosci. Abstr.*, **26**, 353.14.

Zhong, Y., Dunn, P.M., Xiang, Z., Bo, X. & Burnstock, G. (1998) Pharmacological and molecular characterisation of P2X purinoceptors in rat pelvic ganglion neurons. *Br. J. Pharmacol.*, **125**, 771–781.